Motion of the Seawater Interface in Coastal Aquifers: A Numerical Solution

U. SHAMIR AND G. DAGAN

Technion-Israel Institute of Technology, Haifa, Israel

Abstract. The partial differential equations that describe the motion of the seawater interface and the free surface in a phreatic coastal aquifer (or the freshwater head replacing the latter, in the confined case) are presented. They are based on the Dupuit approximation and take into consideration the geometry of the vertical section through the aquifer, in whose plane the flow takes place, as well as the spatial variation of properties of the porous medium and the spatial and temporal distributions of accretion, recharge, and pumping. An implicit numerical scheme is presented to solve the set of simultaneous partial differential equations. The scheme is based on a linearization of the equations and employs a grid with one spacing over the intrusion length and a different spacing in the remainder of the field. Efficient solution of the resulting set of simultaneous linear equations for each time step is achieved by arranging them in a way that results in a 7 diagonal coefficient matrix. Examples are presented, for which the numerical solutions are compared with analytical solutions or laboratory experiments.

The use of coastal aquifers as operational reservoirs in water resource systems requires the development of tools that make it possible to predict the behavior of the aquifer under different conditions. One of the major problems is the prediction of the motion of the saltwater body in the aquifer, due to pumping, artificial recharge, and the varying natural replenishment.

The techniques used so far to solve the problem of the unsteady flow of fresh and salt water in coastal aquifers were approximate analytical techniques and models, primarily the Hele-Shaw model. The analytical methods developed to date apply only to very special, simplified cases. Models are rather expensive to construct and use, and tests made with the models are time consuming.

Pinder and Cooper [1970] recently presented a numerical solution for the moving interface between fresh and salt water in porous media. They solved the two-dimensional problem by considering both the equation of motion and the solute transport equation. Their solution yielded the motion of the saltwater body and the distribution of concentration of the solute for a particular two-dimensional problem. In general the numerical computations under the Pinder-Cooper scheme will probably be lengthy because of the large number of grid points. We also expect difficulties in a narrow transition zone in which there are large concentration gradients.

PROBLEM AND BASIC ASSUMPTIONS

The present work deals with the motion of the interface between fresh and salt waters in a coastal aquifer, which may be either phreatic (Figure 1) or confined (Figure 2). We consider a vertical section through the aquifer, at right angles to the shoreline, and treat the motion as two-dimensional in the plane of this section.

We assume the interface is a well defined line; i.e., we neglect the effect of dispersion between the moving fresh and salt waters that creates a continuous transition over some width from fresh to salt water.

We also adopt the Dupuit assumptions; that is, we assume the hydraulic head along a vertical line in the freshwater zone given by ($\phi^f = p^f/\gamma^f + z$) is constant, and we assume the head along a vertical in the saltwater zone given by ($\phi^s = p^s/\gamma^s + z$) is also constant. These assumptions transform the two-dimensional formulation into a one-dimensional one, in which the dependent variables remain constant in the vertical direction z and change only in x. These assumptions are justified as long as vertical dimensions of the fresh and saltwater flow fields are small when compared to horizontal dimensions. Specifically, the Dupuit approximation is valid as long as the intrusion length L is much larger than the thickness of the aquifer. Even with these simplifying assumptions, one cannot solve the motion of the interface and the phreatic surface analytically, except where the aquifer is confined and of uniform thickness and the interface is a straight line. This solution [*Keulegan*, 1954] is presented in a later section and the results obtained by the numerical scheme are compared with the exact analytical solution. Approximate analytical solutions also exist in a few other instances [*Dagan*, 1964; *Bear and Dagan*, 1964]. However, in practical instances the thickness of the aquifer and the properties of the porous media may vary from point to point. The natural recharge that reaches the freshwater body through accretion may vary both in space and time and wells placed anywhere along the length of the aquifer may follow any prescribed pattern of pumping and recharge; the freshwater discharge that enters the coastal zone from inland may vary in time. Under these general conditions there seems little chance of obtaining even an approximate analytical solution. We therefore resort to a numerical solution.

We retain the Dupuit assumption even though a numerical scheme could be devised to treat the exact two-dimensional formulation. A numerical solution of the full two-dimensional formulation would require a much more complex numerical scheme and more computer time, which do not seem justified because the

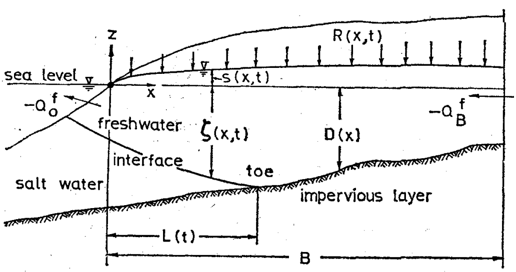

Fig. 1. Vertical section in a phreatic coastal aquifer.

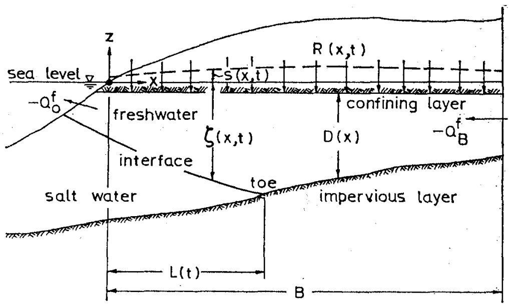

Fig. 2. Vertical section in a confined coastal aquifer.

flow is usually shallow under field conditions and the Dupuit formulation leads to minor errors only. Moreover, the inaccuracies in determining the properties (hydraulic conductivity and effective porosity) of the porous medium and the exact geometry of the bottom layer overshadow the errors that result from using the Dupuit assumptions.

We have used some laboratory experiments, performed with a Hele-Shaw model, to test the numerical scheme. In these experiments the conditions were such that the Dupuit approximation was in appreciable error. Thus the numerical results differed somewhat from the experimental results. This difference will be discussed later in more detail.

THE EQUATIONS

Development of the equations that govern the motion of the phreatic surface and of the interface between the fresh and salt waters in a coastal aquifer has been given in many works [*Bear and Dagan*, 1964].

We give here only the final form that results from writing the continuity equations for each region in which the Dupuit approximation is used. Over the intrusion length $0 \leq x \leq L(t)$ the equations for the fresh and salt water are combined by requiring that the pressure in the two regions be equal at the interface. The resulting equations are:

For $0 \leq x \leq L(t)$

$$\alpha n^f \frac{\partial s}{\partial t} + n^s \frac{\partial \zeta}{\partial t} - \frac{\partial}{\partial x}\left[K^f(\zeta + \alpha s)\frac{\partial s}{\partial x}\right] = R \quad (1)$$

$$n^s \frac{\partial \zeta}{\partial t} + \frac{\partial}{\partial x}$$

$$\cdot \left[K^s(D - \zeta) \frac{\partial}{\partial x} \left(\frac{\gamma^f}{\gamma^s} s - \frac{\Delta\gamma}{\gamma^s} \zeta \right) \right] = 0 \quad (2)$$

For $L(t) \leq x \leq B$

$$\alpha n^f \frac{\partial s}{\partial t} - \frac{\partial}{\partial x} \left[K^f(D + \alpha s) \frac{\partial s}{\partial x} \right] = R \quad (3)$$

where

- $s = s(x, t)$, elevation of the phreatic surface (or hydraulic grade line for a confined aquifer) above sea level;
- $\zeta = \zeta(x, t)$, distance from sea level to the interface;
- n^f, effective porosity for movement of the phreatic surface;
- n^s, effective porosity for movement of the interface;
- $K^f = K^f(x)$, hydraulic permeability in the freshwater zone;
- $K^s = K^s(x)$, hydraulic permeability in the saltwater zone;
- $D = D(x)$, thickness of the aquifer from sea level down to the impervious layer;
- $R = R(x, t)$, net inflow into the aquifer from above (natural replenishment plus artificial recharge minus pumpage);
- γ^f, γ^s, specific weight of fresh and salt water, respectively;
- $\Delta\gamma = \gamma^s - \gamma^f$;
- α, parameter used for generalizing the formulation to include both the phreatic ($\alpha = 1$) and confined ($\alpha = 0$) cases.

The setting of $\alpha = 0$ eliminates those terms from the equations in which s denotes storage or thickness of the flow region of the freshwater, but retains the terms in which s stands for the head in the freshwater.

INITIAL AND BOUNDARY CONDITIONS

As an initial condition we need the location both of the interface ζ and of the phreatic surface s (or, for the confined case, the distribution of the head) at some initial time, which is denoted by t_0

$$\zeta(x, t_0) \qquad 0 \leq x \leq L(t_0) \qquad (4)$$

$$s(x, t_0) \qquad 0 \leq x \leq B \qquad (5)$$

On the seashore ($x = 0$) the Dupuit approximation requires the conditions $s(0, t) = \zeta(0, t) = 0$ for all t. In reality there is a seepage face there; i.e., $s(0, t)$ and $\zeta(0, t)$ have some finite values, but these cannot be determined when the Dupuit approximation is used. One can take them from approximate analytical solutions or laboratory experiments. Thus we assume for the numerical solution that we have such values and write

$$s(0, t) = s_0(t) \qquad t \geq t_0 \qquad (6)$$

$$\zeta(0, t) = \zeta_0(t) \qquad t \geq t_0 \qquad (7)$$

Under field conditions these distributions are unknown. When the interface is shallow one may set $s(0, t) = \zeta(0, t) = 0$ for all t without much error. Another possibility is to adopt the steady solution [*Bear and Dagan,* 1964]

$$\zeta(0, t) = \frac{Q_0^f(t)}{K^f(\Delta\gamma/\gamma^f)} \qquad (8)$$

where $Q_0^f(t)$ is the freshwater discharge leaving the aquifer into the sea (Figure 1). This expression holds when Q_0^f remains constant, and may be used as an approximation when $Q_0^f = Q_0^f(t)$.

The condition at the toe of the interface is

$$\zeta[L(t), t] = D[L(t)] \qquad (9)$$

At the end of the aquifer $x = B$ we may either have an impermeable boundary or a known freshwater discharge crossing it. The boundary condition is

$$Q_B^f = -\left[K^f(D + \alpha s) \frac{\partial s}{\partial x} \right] \Bigg|_{x=B} \qquad (10)$$

where $Q_B^f < 0$ when the flow is toward the sea, i.e., entering the aquifer from inland. When $x = B$ is an impermeable boundary, $Q_B^f = 0$ and the following condition have to be satisfied:

$$\frac{\partial s}{\partial x} \Bigg|_{x=B} = 0 \qquad (11)$$

Boundary conditions 6 to 10 and initial conditions 4 and 5 suffice to enable the solution of equations 1, 2, and 3. An additional boundary condition for equations 1 and 3 is obtained by requiring that $s[L(t), t]$ match from both equations.

The distribution of $R = R(x, t)$ both in time and space is assumed known. For the numerical solution the net result of accretion, pumping, and recharge throughout an element are lumped in R for that element.

NUMERICAL SCHEME

The Grid

For the numerical solution we divide the length of the field into discrete elements (Figure 3). The intrusion length is divided into short elements because a good definition of the location of the interface is of prime importance, and ζ varies quite rapidly (as compared to s) with x. Beyond the toe we tolerate much larger, and thus fewer, elements; therefore the computation is made more efficient. We thus have $(n + 1)$ increments of length Δx_1 each for $0 \leq x \leq L(t)$, and $(m - n)$ increments of length Δx_2 each for $L(t) \leq x \leq B$.

After each time step the toe moves, which establishes a new $L(t)$. At this time a rezoning of the grid is performed by dividing the new intrusion length into $(n + 1)$ equal increments and the remaining length $(B - L(t))$ into $(m - n)$ equal increments, where n and m are fixed. Thus the interface is always defined by the same number of grid points. When the intrusion length is small, and as a result the interface is steep, the grid points are close together. When the position of the interface varies more gradually the grid points are farther apart. If during the solution the intrusion length undergoes major changes, the fixed number of grid points in each zone could result in a very close grid spacing in one region and a very large spacing in the other. We thus limit both Δx_1 and Δx_2 to be between an upper and lower bound. When they reach a bound the number of grid points is changed for the next rezoning.

We denote each grid point by an index i; $i = 0, 1, \cdots, (n + 1)$ for $0 \leq x \leq L(t)$ and

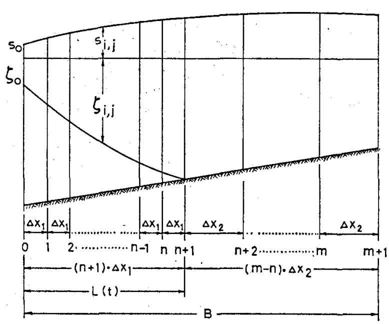

Fig. 3. The grid.

$i = (n + 1), \cdots, (m + 1)$ for $L(t) \leq x \leq B$. The time interval is denoted by an index j, $j = 1, 2, \cdots$. Thus $s_{i,j}$ and $\zeta_{i,j}$ denote the values of s and ζ at the ith grid point, at the end of the jth time interval.

The unknowns at each time step are

$$\zeta_{i,j+1} \qquad i = 1, \cdots, n$$

and

$$s_{i,j+1} \qquad i = 1, \cdots, m$$

for a total of $(n + m)$ unknowns. As we shall show later there are also $(n + m)$ equations, which makes the system of equations solvable.

To simplify the notation we abbreviate average values, for example

$$K_{i+1/2}{}^f \equiv \tfrac{1}{2}(K_i{}^f + K_{i+1}{}^f)$$

$$\zeta_{i-1/2,j} \equiv \tfrac{1}{2}(\zeta_{i-1,j} + \zeta_{i,j})$$

$$R_{i,j+1/2} \equiv \tfrac{1}{2}(R_{i,j} + R_{i,j+1})$$

Note also that although no time index appears for D, K^f and K^s, the locations at which they are needed, i.e., the grid points, move with each time step as a result of the rezoning. An interpolation procedure is used after rezoning to compute the above quantities, as well as s, ζ, and R at the new grid points.

Implicit versus Explicit Scheme

The simplest way to write a difference analog of the partial differential equations would be to use an explicit formulation. In such a formulation unknowns appear only in time derivatives. For example, $\partial s/\partial t$ would be written $(s_{i,j+1} - s_{i,j})/\Delta t$. The spatial derivatives would all be expressed in terms of (known) values at the old time. For example, $\partial s/\partial x$ at the ith point could be expressed as $(s_{i+1,j} - s_{i-1,j})/2\Delta x$. The equations that result from an explicit formulation are solved one at a time and are independent of the other equations; this leads to an extremely simple algorithm, but has a major limitation. It can be shown that such a scheme is unstable unless the spatial and temporal increments satisfy a stability criterion.

The problem under consideration is not linear, and therefore only an approximate stability criterion can be formulated. Consider equation 2, in which the temporal derivative is of ζ. If one neglects the change in $K^s(D - \zeta)$ with x we get

$$n^s \frac{\partial \zeta}{\partial t} + K^s(D - \zeta)\left(\frac{\gamma^f}{\gamma^s}\frac{\partial^2 s}{\partial x^2} - \frac{\Delta\gamma}{\gamma^s}\frac{\partial^2 \zeta}{\partial x^2}\right) = 0 \tag{12}$$

The curvature of the free surface is usually negligible when compared with that of the interface. If we drop it from the equation, we are left with

$$\frac{\partial \zeta}{\partial t} - \left[\frac{K^s(D - \zeta)\,\Delta\gamma}{n^s\gamma^s}\right]\frac{\partial^2 \zeta}{\partial x^2} = 0 \tag{13}$$

If we assume the term in brackets is constant we have the following stability criterion from the well-known theory for linear equations:

$$\frac{K^s(D - \zeta)\,\Delta\gamma}{n^s\gamma^s}\frac{\Delta t}{(\Delta x)^2} \le \frac{1}{2} \tag{14}$$

The restriction is most severe when $(D - \zeta)$ is as large as possible. Let us take $(D - \zeta) = D/2$, say, a reasonable average value in field conditions. For the following data:

$$K^s = 40 \text{ m/day} \qquad n^s = 0.2$$

$$\Delta\gamma/\gamma^s = 0.03 \qquad D = 100 \text{ meters}$$

we get

$$\frac{\Delta t}{(\Delta x)^2} \le \frac{1}{2}\frac{0.2}{40 \times 25 \times 0.03} = \frac{1}{300} \tag{15}$$

If we take $\Delta x = 50$ meters$(=D/2)$, which is a rather large value, this requires

$$\Delta t \le 8.3 \text{ days} \tag{16}$$

The motion of the interface over appreciable distances is a matter of several years. Condition 16 would lead to an impractical number of time steps, even if we allowed a somewhat higher value on the right-hand side of condition 14.

Consequently we adopt the implicit scheme, which although more laborious at each step is unconditionally stable.

Linearization

The differential equations are nonlinear because they include products of variables and their derivatives. One could write nonlinear implicit difference equations in which the values of s and ζ both in the coefficients and in the derivatives would appear at the new time, i.e., as unknowns. One has then to solve at each time step of $(n + m)$ simultaneous nonlinear algebraic equations. The solution, obtained by some suitable iterative technique, would require a prohibitively large amount of computer time.

We have thus elected to linearize the equations as follows: in all spatial derivatives s and ζ will appear at the new time $(j + 1)$, i.e., as unknowns, whereas in all other places they will appear as known values from the old time j. We have also provided for an iterative scheme in the computer program, which proceeds in the following way. With the 'old' values of $s_{i,j}$ and $\zeta_{i,j}$ one solves the unknowns $s_{i,j+1}$ and $\zeta_{i,j+1}$. Then for the same time step one updates the values in the coefficients by using the most recently calculated values of s and ζ, and repeats the solution. These iterations are continued until values of the unknowns on successive iterations are within some prescribed accuracy tolerance. The user can also specify the number of iterations to be performed at each time step, regardless of the convergence achieved.

DIFFERENCE EQUATIONS AND THEIR SOLUTIONS

The finite difference scheme is based on equation 1 (continuity in the freshwater above the interface), equation 2 (continuity in the salt water), and equation 3 (continuity in the freshwater beyond the toe).

Equation 1

For $i = 2, \cdots, n$. A linear equation in the unknowns

$$\alpha n^f \frac{s_{i,j+1} - s_{i,j}}{\Delta t} + n^s \frac{\zeta_{i,j+1} - \zeta_{i,j}}{\Delta t} - K_{i+1/2}{}^f(\zeta_{i+1/2,j} + \alpha s_{i+1/2,j}) \cdot \frac{s_{i+1,j+1} - s_{i,j+1}}{(\Delta x_1)^2} + K_{i-1/2}{}^f(\zeta_{i-1/2,j} + \alpha s_{i-1/2,j}) \cdot \frac{s_{i,j+1} - s_{i-1,j+1}}{(\Delta x_1)^2} = R_{i,j+1/2} \tag{17}$$

may be written in the following form

$$A_{i,j}s_{i-1,j+1} + B_{i,j}s_{i,j+1} + C_{i,j}s_{i+1,j+1} + P_{i,j}\zeta_{i,j+1} = M_{i,j} \quad (18)$$

where the coefficients are

$$A_{i,j} = \frac{-\Delta t}{(\Delta x_1)^2} K_{i-1/2}{}^f(\zeta_{i-1/2,j} + \alpha s_{i-1/2,j}) \quad (19)$$

$$B_{i,j} = \alpha n^f - A_{i,j} - C_{i,j} \quad (20)$$

$$C_{i,j} = \frac{-\Delta t}{(\Delta x_1)^2} K_{i+1/2}{}^f(\zeta_{i+1/2,j} + \alpha s_{i+1/2,j}) \quad (21)$$

$$P_{i,j} = n^s \quad (22)$$

$$M_{i,j} = \Delta t R_{i,j+1/2} + \alpha n^f s_{i,j} + n^s \zeta_{i,j} \quad (23)$$

For $i = 1$. At the sea ($i = 0$) we have the boundary condition

$$\left.\begin{aligned} s_{i-1,j} &= s_{0,j} \\ \zeta_{i-1,j} &= \zeta_{0,j} \end{aligned}\right\} \quad j = 0, 1, 2, \cdots$$

and thus

$$A_{1,j} = \frac{-\Delta t}{(\Delta x_1)^2} \cdot K_{1/2}{}^f\left(\frac{\zeta_{0,j} + \zeta_{1,j}}{2} + \alpha \frac{s_{0,j} + s_{1,j}}{2}\right) \quad (24)$$

The other coefficients are given by equations 20 to 22, where in equation 20 for $B_{1,j}$ we use the value for $A_{1,j}$ from equation 24. As $s_{0,j+1}$ is known (as a boundary condition) it does not appear on the left-hand side of equation 18, and the product $A_{1,j} \cdot s_{0,j+1}$ is transferred to the right-hand side to yield

$$M_{1,j} = \Delta t R_{1,j+1/2} + \alpha n^f s_{1,j} + n^s \zeta_{1,j} - A_{1,j}s_{0,j+1} \quad (25)$$

For $i = n + 1$. Here the grid spacing changes from Δx_1 to Δx_2, and also $\zeta_{n+1,j} = D_{n+1}$

$$\alpha n^f \frac{s_{n+1,j+1} - s_{n+1,j}}{\Delta t} + n^s \frac{\zeta_{n+1,j+1} - D_{n+1}}{\Delta t} - K_{n+3/2}{}^f(D_{n+3/2} + \alpha s_{n+3/2,j}) \cdot \frac{s_{n+2,j+1} - s_{n+1,j+1}}{\Delta x_2(\Delta x_1 + \Delta x_2)/2} + K_{n+1/2}{}^f\left(\frac{D_{n+1} + \zeta_{n,j}}{2} + \alpha s_{n+1/2,j}\right) \cdot \frac{s_{n+1,j+1} - s_{n,j+1}}{\Delta x_1(\Delta x_1 + \Delta x_2)/2} = R_{n+1,j+1/2} \quad (26)$$

We again have a linear equation of the form given by (18), this time with coefficients given by

$$A_{n+1,j} = \frac{-2\Delta t}{\Delta x_1(\Delta x_1 + \Delta x_2)} \cdot K_{n+1/2}{}^f\left(\frac{D_{n+1} + \zeta_{n,j}}{2} + \alpha s_{n+1/2,j}\right) \quad (27)$$

$$B_{n+1,j} = \alpha n^f - A_{n+1,j} - C_{n+1,j} \quad (28)$$

$$C_{n+1,j} = \frac{-2\Delta t}{\Delta x_2(\Delta x_1 + \Delta x_2)} \cdot K_{n+3/2}{}^f(D_{n+3/2} + \alpha s_{n+3/2,j}) \quad (29)$$

$$M_{n+1,j} = \Delta t R_{n+1,j+1/2} + \alpha n^f s_{n+1,j} + n^s \zeta_{n+1,j} \quad (30)$$

However, ζ should not be an unknown at $i = n + 1$. For reasons to be explained in the next section, we express the unknown $\zeta_{n+1,j+1}$ in terms of the unknowns $\zeta_{n-1,j+1}$ and $\zeta_{n,j+1}$ by using the following linear extrapolation:

$$\zeta_{n+1,j+1} = 2\zeta_{n,j+1} - \zeta_{n-1,j+1}$$

When this expression is inserted into equation 18 for $i = n + 1$ the following terms appear

$$-P_{n+1,j}\zeta_{n-1,j+1} + 2P_{n+1,j}\zeta_{n,j+1}$$

where

$$P_{n+1,j} = n^s \quad (31)$$

Equation 2

For $i = 2, \cdots, (n - 1)$. A linear equation in the unknowns

$$n^s \frac{\zeta_{i,j+1} - \zeta_{i,j}}{\Delta t} + K_{i+1/2}{}^s(D_{i+1/2} - \zeta_{i+1/2,j}) \cdot \frac{\frac{\gamma^f}{\gamma^s}(s_{i+1,j+1} - s_{i,j+1}) - \frac{\Delta\gamma}{\gamma^s}(\zeta_{i+1,j+1} - \zeta_{i,j+1})}{(\Delta x_1)^2} - K_{i-1/2}{}^s(D_{i-1/2} - \zeta_{i-1/2,j}) \cdot \frac{\frac{\gamma^f}{\gamma^s}(s_{i,j+1} - s_{i-1,j+1}) - \frac{\Delta\gamma}{\gamma^s}(\zeta_{i,j+1} - \zeta_{i-1,j+1})}{(\Delta x_1)^2} = 0 \quad (32)$$

can be put in the following form:

$$E_{i,j}s_{i-1,j+1} + F_{i,j}s_{i,j+1} + G_{i,j}s_{i+1,j+1} + H_{i,j}\zeta_{i-1,j+1} + I_{i,j}\zeta_{i,j} + J_{i,j}\zeta_{i+1,j+1} = N_{i,j} \qquad (33)$$

The coefficients are given by:

$$E_{i,j} = \frac{\Delta t}{(\Delta x_1)^2} K_{i-1/2}^s(D_{i-1/2} - \zeta_{i-1/2,j}) \frac{\gamma^f}{\gamma^s} \qquad (34)$$

$$F_{i,j} = -E_{i,j} - G_{i,j} \qquad (35)$$

$$G_{i,j} = \frac{\Delta t}{(\Delta x_1)^2} K_{i+1/2}^s(D_{i+1/2} - \zeta_{i+1/2,j}) \frac{\gamma^f}{\gamma^s} \qquad (36)$$

$$H_{i,j} = \frac{-\Delta t}{(\Delta x_1)^2} K_{i-1/2}^s(D_{i-1/2} - \zeta_{i-1/2,j}) \frac{\Delta\gamma}{\gamma^s} = -E_{i,j} \frac{\Delta\gamma}{\gamma^f} \qquad (37)$$

$$I_{i,j} = n^s - H_{i,j} - J_{i,j} \qquad (38)$$

$$J_{i,j} = \frac{-\Delta t}{(\Delta x_1)^2} K_{i+1/2}^s(D_{i+1/2} - \zeta_{i+1/2,j}) \frac{\Delta\gamma}{\gamma^s} = -G_{i,j} \frac{\Delta\gamma}{\gamma^f} \qquad (39)$$

$$N_{i,j} = n^s \zeta_{i,j} \qquad (40)$$

For $i = 1$. At the sea ($i = 0$) the boundary conditions are

$$\left.\begin{aligned} s_{i-1,j} &= s_{0,j} \\ \zeta_{i-1,j} &= \zeta_{0,j} \end{aligned}\right\} \qquad j = 0, 1, 2, \cdots \qquad (41)$$

and thus

$$E_{1,j} = \frac{\Delta t}{(\Delta x_1)^2} K_{1/2}^s\left(D_{1/2} - \frac{\zeta_{0,j} + \zeta_{1,j}}{2}\right) \frac{\gamma^f}{\gamma^s} \qquad (42)$$

The other coefficients are given by equations 35 to 39 where in equation 35 for $F_{1,j}$ one uses $E_{1,j}$ from equation 42. Also, since $\zeta_{0,j+1}$ and $s_{0,j+1}$ are given they do not appear as unknowns, and the products $E_{1,j}\, s_{0,j+1}$ and $H_{1,j}\, \zeta_{0,j+1}$ are transferred to the right-hand side to yield

$$N_{1,j} = n^s \zeta_{1,j} - E_{1,j}s_{0,j+1} - H_{1,j}\zeta_{0,j+1} \qquad (43)$$

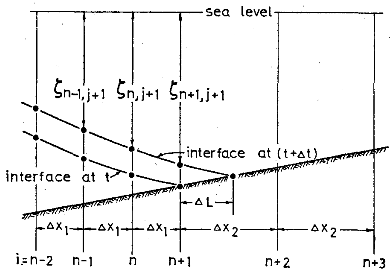

Fig. 4. Motion of the toe (advancing inland).

For $i = n$. This is the toe of the interface, where the saltwater wedge becomes very narrow. It was discovered that the method for treating this zone has a major influence on the resulting motion of the toe. Figure 4 describes the zone under consideration. The grid shown is the one established after having computed the solution at time t, which is then used for the computation during the next Δt. When writing the equation of continuity in the salt water at $i = n$ the value of the unknown $\zeta_{n+1,j+1}$ appears in the equation. We could have assumed that if the time step is not too large, no great error is introduced if one neglects the change at point $(n + 1)$ with time, and writes $\zeta_{n+1,j+1} = \zeta_{n+1,j} = D_{n+1}$. It turns out, however, that as the whole saltwater zone is rather narrow, this simplification does have a significant effect on the movement of the toe, even though the rest of the interface is computed correctly. As the exact location of the toe is of major practical importance, a more refined method is adopted. Even though the change in ζ_{n+1} is not neglected, it has to be expressed in terms of other unknown values of ζ to keep the number of unknowns equal to the number of available equations. The straight line extrapolation

$$\zeta_{n+1,j+1} = \zeta_{n,j+1} + (\zeta_{n,j+1} - \zeta_{n-1,j+1}) = 2\zeta_{n,j+1} - \zeta_{n-1,j+1} \qquad (44)$$

proved satisfactory. When this expression is introduced into equation 32 for $i = n$, equation 33 takes on the form

$$E_{n,j}s_{n-1,j+1} + F_{n,j}s_{n,j+1} + G_{n,j}s_{n+1,j+1} + (H_{n,j} - J_{n,j})\zeta_{n-1,j+1} + (I_{n,j} + 2J_{n,j})\zeta_{n,j+1} = N_{n,j} \qquad (45)$$

with the coefficients given by equation 34 to equation 40.

The New Position of the Toe

The movement of the toe ΔL during the time interval Δt is computed by intersecting two straight lines:

1. Through the points $\zeta_{n-1,\,j+1}$ and $\zeta_{n,\,j+1}$

$$\zeta(x) = \zeta_n + \frac{\zeta_n - \zeta_{n-1}}{\Delta x_1}(x - x_n)$$

2. Through the points D_n and D_{n+1}

$$D(x) = D_{n+1} + \frac{D_{n+1} - D_n}{\Delta x_1}(x - x_{n+1})$$

which intersect at $x = x_{n+1} + \Delta L = x_n + \Delta x_1 + \Delta L$. Through the solution of ΔL one obtains

$$\Delta L = \left(\frac{D_{n+1} + \zeta_{n-1} - 2\zeta_n}{\zeta_n - \zeta_{n-1} + D_n - D_{n+1}}\right)\Delta x_1 \quad (46)$$

Equation 3

For $i = (n+2), \cdots, (m-1)$. A linear equation in the unknowns

$$\alpha n^f \frac{s_{i,j+1} - s_{i,j}}{\Delta t} - K_{i+1/2}{}^f(D_{i+1/2} + \alpha s_{i+1/2,j}) \cdot \frac{s_{i+1,j+1} - s_{i,j+1}}{(\Delta x_2)^2} + K_{i-1/2}{}^f(D_{i-1/2} + \alpha s_{i-1/2,j}) \cdot \frac{s_{i,j+1} - s_{i-1,j+1}}{(\Delta x_2)^2} = R_{i,j+1/2} \quad (47)$$

can be written in the form

$$A_{i,j}s_{i-1,j+1} + B_{i,j}s_{i,j+1} + C_{i,j}s_{i+1,j+1} = M_{i,j} \quad (48)$$

with the coefficients given by

$$A_{i,j} = \frac{-\Delta t}{(\Delta x_2)^2} K_{i-1/2}{}^f(D_{i-1/2} + \alpha s_{i-1/2,j}) \quad (49)$$

$$B_{i,j} = \alpha n^f - A_{i,j} - C_{i,j} \quad (50)$$

$$C_{i,j} = \frac{-\Delta t}{(\Delta x_2)^2} K_{i+1/2}{}^f(D_{i+1/2} + \alpha s_{i+1/2,j}) \quad (51)$$

$$M_{i,j} = \Delta t R_{i,j+1/2} + \alpha n^f s_{i,j} \quad (52)$$

For $i = n + 1$. One obtains equation 26, where the unknowns are $s_{n,\,j+1}$, $s_{n+1,\,j+1}$, and $s_{n+2,\,j+1}$. Equation 47 is then written for $i = (n+2), \cdots, (m-1)$. The solution of all the equations is performed simultaneously, as will be explained later, and thus the solutions of equations 26 and 47 for s are made to match at $i = n + 1$.

For $i = m$. The continuity equation for the last element of the field has to take into consideration the freshwater discharge entering the field from inland $(-Q_B{}^f)$.

The equation is

$$\alpha n^f \frac{s_{m,j+1} - s_{m,j}}{\Delta t} + K_{m-1/2}{}^f(D_{m-1/2} + \alpha s_{m-1/2,j}) \cdot \frac{s_{m,j+1} - s_{m-1,j+1}}{\Delta x_2} = R_{m,j+1/2} - Q_B{}^f \quad (53)$$

which can be written as

$$A_{m,j}s_{m-1,j+1} + B_{m,j}s_{m,j} = M_{m,j} \quad (54)$$

with the coefficients given by

$$A_{m,j} = \frac{-\Delta t}{(\Delta x_2)} K_{m-1/2}{}^f(D_{m-1/2} + \alpha s_{m-1/2,j}) \quad (55)$$

$$B_{m,j} = \alpha n^f - A_{m,j} \quad (56)$$

$$M_{m,j} = \Delta t R_{m,j+1/2} - \Delta t Q_B{}^f + \alpha n^f s_{m,j} \quad (57)$$

The discharge $Q_B{}^f$ can be expressed by Darcy's law as

$$Q_B{}^f = -K_{m+1/2}{}^f(D_{m+1/2} + \alpha s_{m+1/2,j}) \cdot \frac{s_{m+1,j+1} - s_{m,j+1}}{\Delta x_2} \quad (58)$$

One can thus compute $s_{m+1,j+1}$, to be used in the next time step, from

$$s_{m+1,j+1} = s_{m,j+1} + \frac{\Delta x_2 Q_B{}^f}{K_{m+1/2}{}^f(D_{m+1/2} + s_{m+1/2,j})} \quad (59)$$

Solution of the Set of Simultaneous Linear Equations

The solution of the set of simultaneous equations can be made most efficient by arranging the $(m + n)$ unknowns in a way that yields a compactly banded coefficient matrix. The arrangement selected is seen in Figure 5. The

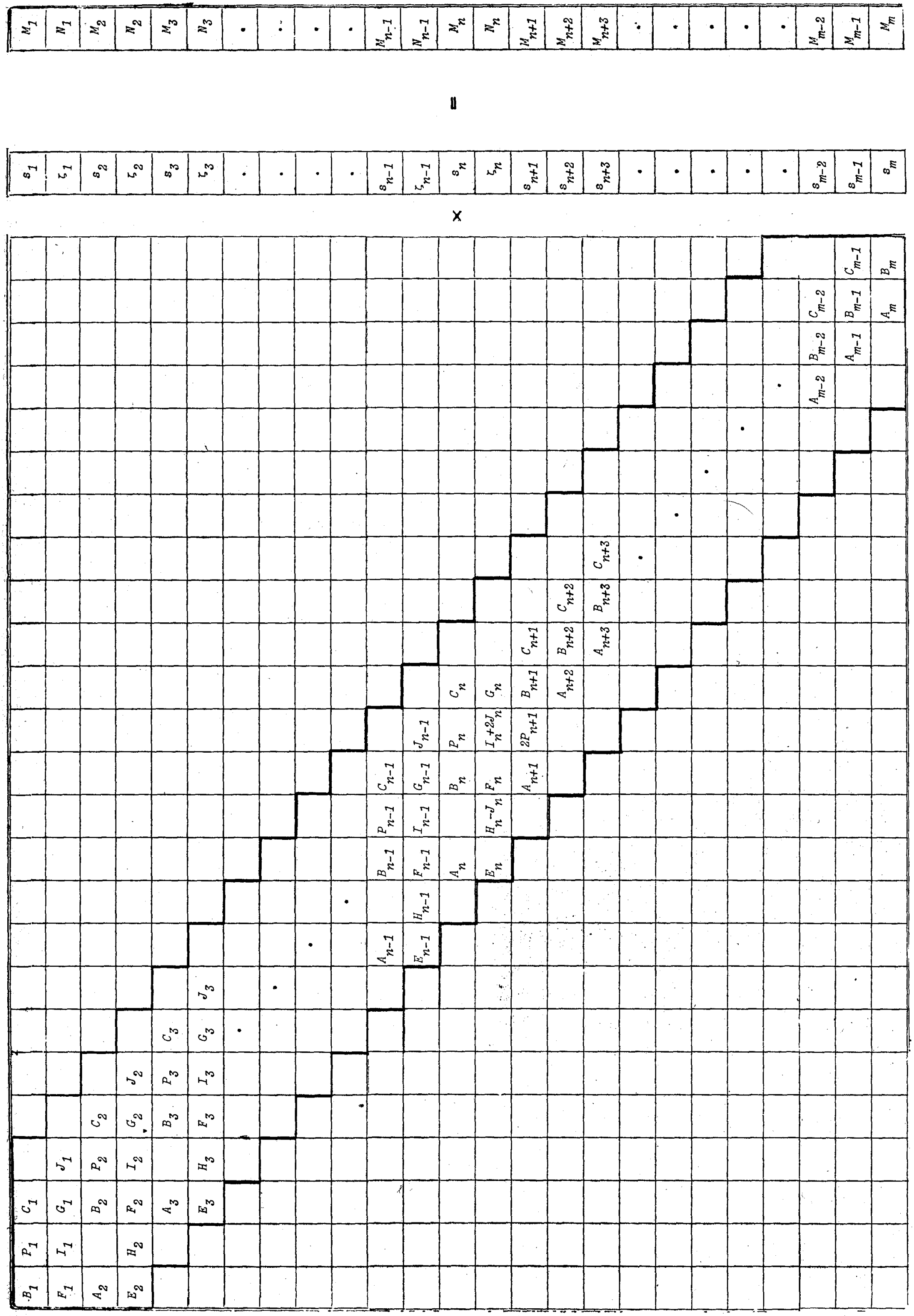

Fig. 5. The set of simultaneous equations.

resulting coefficient matrix is treated as a 7 diagonal matrix, and the fact that some of the coefficients in this band are identically zero is ignored. The solution of the resulting equations was obtained with a standard computer program.

The coefficient matrix is well behaved, and roundoff errors do not present a problem, even with standard accuracy operations.

Interpolation

After each time step a rezoning of the grid is performed. For the new grid one has to compute the values of D, K^f, K^s, R, ζ, and s at the new grid points. This is done by interpolation, using the values at the old grid points. A simple three-point interpolation procedure was used throughout, except near the toe and at ends of the field ($x = 0$ and $x = B$). Near the toe the grid spacing changes, and a special procedure was developed to ensure that the description of s in the new grid was smooth (i.e., more than three points were used). Near the ends of the field a two-point interpolation was used.

SAMPLE PROBLEMS

Linear Interface

Consider a confined aquifer of uniform thickness, as shown in Figure 6. At time $t = 0$ there is a vertical interface at $x = 0$, with salt water in the part $x < 0$ and freshwater in $x > 0$. This condition is maintained by a vertical gate, say located at $x = 0$. At $t = 0_+$ the gate is removed, and the interface begins to move owing to the density difference.

Keulegan [1954] gave an analytical solution for the motion of the interface

$$\zeta(x, t) = \frac{D}{2}\left\{1 + \frac{x}{[(\Delta\gamma K^f\ Dt)/(n\gamma^f)]^{1/2}}\right\} \quad (60)$$

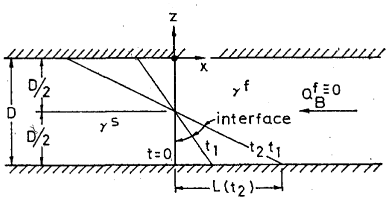

Fig. 6. Linear interface.

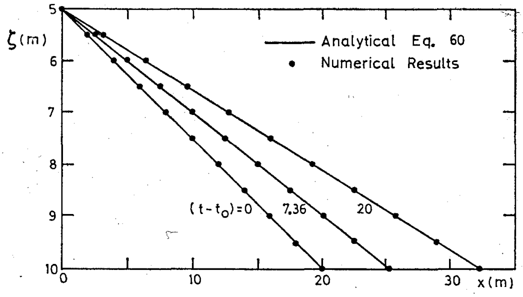

Fig. 7. Comparison between analytical and computed shapes of the linear interface.

The location of the toe is given for $\zeta = D$

$$L(t) = \left(\frac{\Delta\gamma K^f\ D}{n\gamma^f}\right)^{1/2} t^{1/2} = At^{1/2} \quad (61)$$

where A is constant. The potential in the freshwater s is given by

$$s(x, t) = \frac{-n}{4K^f t}\left[\frac{x^2}{2} + L(t)\cdot x + \frac{L^2(t)}{2}\right] + \frac{\Delta\gamma\ D}{2\gamma^f}\left[1 + \frac{x}{L(t)}\right] \quad (62)$$

with $L(t)$ given in equation 61. As can be seen from equation 60, the interface remains linear at all times, and always passes through ($x = 0, z = -D/2$). We thus applied the numerical solution to the part $x \geq 0$ only, maintaining $\zeta(0, t) = D/2$ at all times.

The data used were:

$B = 100$ meters $D = 10$ meters

$\gamma^f = 1.0$ $K^f = 39.024$ m/day

$\gamma^s = 1.025$ $K^s = 40$ m/day

$\Delta\gamma = 0.025$ $n = 0.3$

The solution was started with a linear interface ending at $L(t_0) = 20$ meters, which was then allowed to move. This value of L corresponds to $t_0 = 12.28$ days, as computed from equation 61. The Δt were computed by the program, keeping the movement of $L(t)$ during any Δt to less than one spatial increment Δx_1. Grid data for the numerical solution were $n = 10$, $m = 35$, and the program was run until

$t - t_0 = 20$ days. Figure 7 shows the linear solution for a few times, and Figure 8 shows the progress of the toe as compared with the exact solution (equation 61).

The interface retains its exact linear form, and the toe moves exactly at the theoretical rate. An examination of the values of s computed by the program with the values predicted by equation 62 shows the same degree of agreement.

Hele-Shaw Experiments

The comparison between the numerical solution and the exact solution described in the preceding section referred to the extremely simple case of a linear interface. Our next step was the numerical computation of more complex cases. For this purpose we have considered two of the Hele-Shaw experiments reported by *Bear and Dagan* [1964], which they labeled experiment 1 and experiment 3. In these experiments the interface began in a fixed position maintained by a constant freshwater discharge $Q_B{}^f$ $(t = 0_-)$. At $t = 0_+$ the discharge was abruptly changed to $Q_B{}^f(t = 0_+)$ and was maintained constant afterward. Since the model was confined, the same discharge change occurred simultaneously at the interface toe. The pertinent data are:

	Experiment 1	Experiment 3
D (cm)	27	27
K^f (cm/sec)	69	69
$(\gamma^s - \gamma^f)/\gamma^f$	0.029	0.029
$Q_B{}^f(t = 0_-)$ (cm²/sec)	−19.1	− 3.9
$Q_B{}^f(t = 0_+)$ (cm²/sec)	0	−18.8

D(cm) is aquifer thickness, K^f(cm/sec) is hydraulic conductivity, and $(\gamma^s - \gamma^f)/\gamma^f$ is relative density difference.

The additional input data for the numerical procedure were the distributions of ζ and s at $t = 0$ as well as $\zeta(0, t)$ and $s(0, t)$, which were taken from *Bear and Dagan* [1964, Figure 7].

In the numerical solution of experiment 1 of an inland moving interface, we have taken $B = 200$ cm, $m = 30$, and $n = 13$. Δt was varied as follows:

Δt, sec	t, sec
5	30–45
10	45–90
15	90–165
20	165–225
30	225–525

In Figure 9 we give the curves $L(t)$ of the toe inland movement. The numerical solution

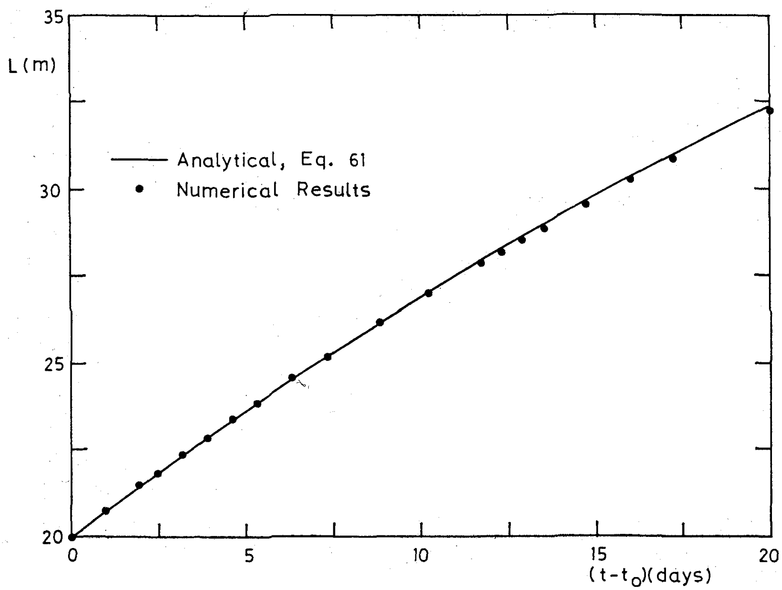

Fig. 8. Motion of the toe of the linear interface.

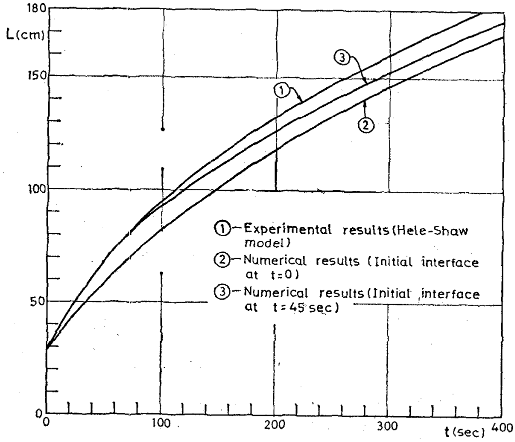

Fig. 9. Motion of the interface toe (experiment 1, moving inland).

(curve 2) shows a lag of the computed toe behind the measured one (curve 1). This distance lag develops at the beginning of the motion ($0 < t < 80$ sec) and remains constant afterward. The ratio $(L_{computed} - L_{experimental})/L_{exp}$ becomes small as the time increases (0.8% for $t = 400$ sec).

Because the seepage face $\zeta(0, t)$ was large at the beginning of the motion, we suspected a deviation from the Dupuit assumption as being the cause of the discrepancy between the numerical and experimental results. For this reason we took the interface at $t = 45$ sec as the initial interface position and reran the program. The result for $L(t)$ (curve 3, Figure 9) showed a much better agreement between the experiment and the computations. Obviously, should we have started at a later stage when the seepage face was negligible, the agreement would have been even better.

In Figure 10 we give the shape of the computed interface at a few times (dashed lines). The striking result is the absence of the inflection point of the computed interface profile.

In the numerical solution of experiment 3 of a seaward moving interface, we have taken $B = 180$ cm, $m = 25$, and $n = 20$. Δt was 5 sec for $t < 20$ sec and $\Delta t = 10$ sec for $t > 20$ sec. A retreating interface needs special care to select the space and time intervals, so that the toe should not move more than Δx_1 in Δt; otherwise the mass balance in the nth cell becomes inaccurate.

In Figure 11 we give the graphs of the toe motion from the experimental data (curve 1) and from the computations.

At the beginning, when the interface slope is mild, the agreement is good. As the interface moves toward the sea, the interface slope and the seepage face become large and the agreement becomes poor. Ultimately, for very large times, near equilibrium, the discrepancy decreases.

Some computed profiles are given in Figure 10. The order of magnitude of the time spent in running each program on the Elliott 503 computer was a few minutes. This time includes reading the program from paper tape, compiling it, reading in the data, and running and printing all the results. The lack of an internal timer made it impossible to measure net running times.

DISCUSSION OF RESULTS

In the preceding sections we have given the results of the numerical solution of a few examples of moving interfaces. In these examples we have assigned the time intervals Δt for reasonably selected space intervals Δx_1 and Δx_2 so that the motion of the toe ΔL would not be larger than Δx_1 during any Δt. In actual problems a special routine has to be provided to enforce this condition. Because our purpose was to test the program at this stage, we took Δt according to the known rate of advance of the toe.

The seepage face dimension $\zeta(0, t)$ has also been borrowed from the experimental results. Again, in applications one has to neglect the seepage face in the case of a large L (say $L > 2\ D$) or to take it from empirical results.

The numerical results were in very good agreement with the exact solution of a linear interface, which shows that the numerical procedure is essentially accurate.

The comparison between the numerical solutions and the Hele-Shaw experiments reveals a few facts that could not be discovered previously. First, it seems that the inflection point of an inland moving interface, which appeared in experiments, is a two-dimensional effect not reproduced by a solution based on Dupuit assumptions.

A second effect that deserves further analysis is the discrepancy between numerical and

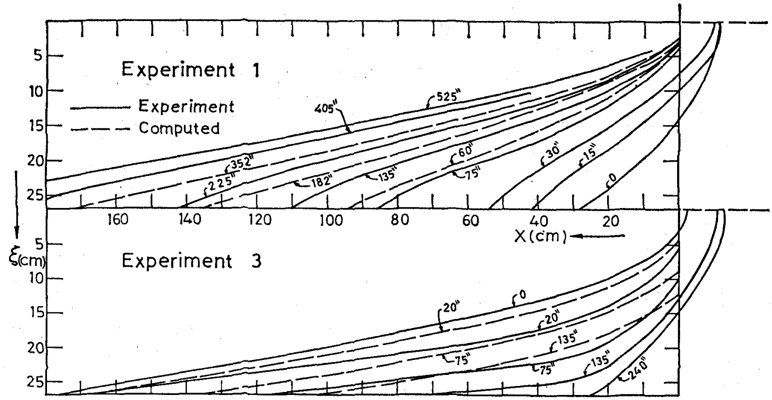

Fig. 10. Comparison between the measured and computed shapes of the moving interface Hele-Shaw experiments.

experimental results when the seepage face is relatively large, irrespective of the intrusion length (experiment 3). The examination of experiment 3 shows a very rapid increase of the seepage face, much more than we should expect from steady state results. This effect, which is nonlinear and not considered by the Dupuit assumptions, probably causes the discrepancy between computations and experiments.

It is probable, however, that in conditions of a continuous, rather than an abrupt change of the freshwater discharge and of a shallow interface ($L \gg D$), the solution based on the Dupuit assumption will produce accurate results.

CONCLUSIONS

The two-dimensional motion of a shallow interface in a coastal aquifer of varying thickness and properties, in the presence of any pattern of recharge and pumping, has been solved numerically. The numerical scheme is stable and provides results in good agreement with an exact solution of a simple case and in fair agreement with experimental findings on a Hele-Shaw model.

The sizes of the space cells and time intervals

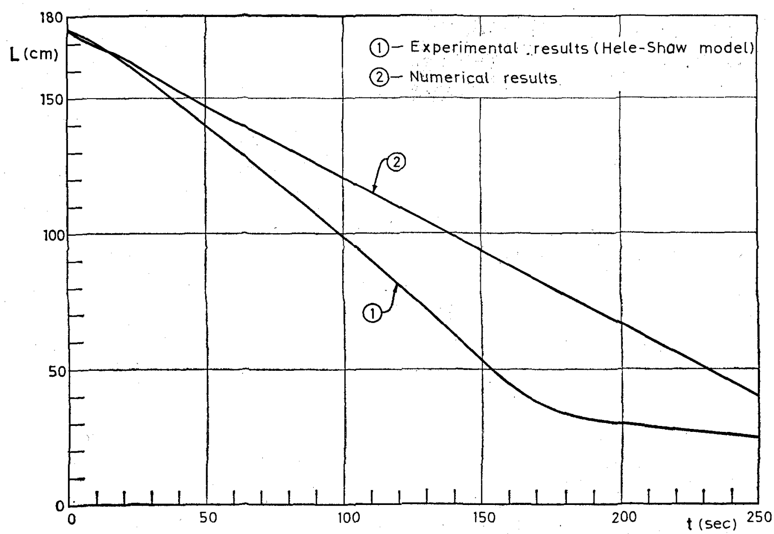

Fig. 11. Motion of the interface toe (experiment 3, moving seaward).

in the program have to be selected so that the interface toe remains within one cell during a time interval. In the present work this condition has been satisfied by an a priori estimate of the toe motion. In a general case, if such an estimate is missing, a trial and error procedure can be used.

The height of the seepage face, which appears in the seaside boundary condition, is generally unknown.

For a shallow interface the seepage face may be taken zero without much error. Another possibility is to adopt the steady state value [*Bear and Dagan,* 1964]

$$\zeta(0, t) = \frac{Q^f(0, t)}{K^f(\Delta\gamma/\gamma^f)}$$

Details on the computer program (written in Algol for the Elliott 503 computer) and on its use are given in *Shamir and Dagan* [1970].

Acknowledgments. The work was supported in part by Technion, under grant 012-300, and in part by Tahal, Water Planning for Israel, Ltd. Thanks are due to Mr. Y. Golan, who wrote, tested, and ran the computer program, and was very helpful in discussing the computational aspects of the work.

REFERENCES

Bear, J., and G. Dagan, Moving interface in coastal aquifers, *J. Hydraul. Div., Amer. Soc. Civil Eng., 90*(HY4), 193–216, 1964.

Dagan, G., The movement of the interface between two liquids in a porous medium with applications to a coastal collector, (in Hebrew with an abstract in English), D.Sc. thesis, Faculty of Civil Engineering, Technion, Haifa, Israel, 1964.

Dagan, G., Computation of the motion of the interface in a coastal aquifer by a numerical scheme, (in Hebrew), 18 pp., Technion Research and Development Foundation Ltd., Haifa, Israel, 1967.

Keulegan, H. G., An example report on model laws for density currents, U.S. National Bureau of Standards, Gaithersburg, Maryland, 1954.

Pinder, G. F., and H. H. Cooper, Jr., A numerical technique for calculating the transient position of the saltwater front, *Water Resour. Res., 6*(3), 875–882, 1970.

Shamir U., and G. Dagan, Motion of the seawater interface in a coastal aquifer: A numerical solution, *Rep. 6/70,* Water Resources Laboratories, Technion, Haifa, Israel, 1970.

(Manuscript received January 4, 1971;
revised March 4, 1971.)